Start-up and Dynamic Analysis of a Novel Thermally Coupled Reactor for the Simultaneous Production of Methanol and Benzene

ARTICLE *in* INDUSTRIAL & ENGINEERING CHEMISTRY RESEARCH · OCTOBER 2011

Impact Factor: 2.59 · DOI: 10.1021/ie201090b

3 AUTHORS, INCLUDING:

M. R. Rahimpour
Shiraz University
331 PUBLICATIONS **3,012** CITATIONS

SEE PROFILE

I&EC research
Industrial & Engineering Chemistry Research

ARTICLE

pubs.acs.org/IECR

Start-up and Dynamic Analysis of a Novel Thermally Coupled Reactor for the Simultaneous Production of Methanol and Benzene

Mohammad Hasan Khademi,[†] Mohammad Reza Rahimpour,*[,†,‡] and Abdolhossein Jahanmiri[†,‡]

[†]Department of Chemical Engineering, School of Chemical and Petroleum Engineering, and [‡]Gas Refining Center of Excellence, Shiraz University, Shiraz 71345, Iran

ABSTRACT: Coupling energy intensive endothermic reaction systems with suitable exothermic reactions improves the thermal efficiency of processes, achieving the autothermality within the reactor, reducing the size of the reactors, and achieving a multiple reactants−multiple products configuration. In this study, a dynamic heterogeneous model for a novel thermally coupled reactor—containing methanol synthesis reactions and cyclohexane dehydrogenation—is developed to consider the startup and transient response of the system. This heat-exchanger reactor consists of two fixed beds separated by a wall, where heat is transferred across the surface of tube from the exothermic side to the endothermic side. The proposed model was validated against conventional methanol synthesis reactor, and a good agreement was achieved. Dynamic simulation results for the co-current mode have been investigated to present the response of the reactor outlet temperature, methanol yield, and cyclohexane conversion in the cases of a step change in the initial molar flow rate and inlet temperature of both sides. The challenges posed by the transient operation of thermally coupled reactor are identified to avoid severe issues that can arise in the course of operating the reactor (such as reactor extinction). The results suggest that control of this coupled reactor could be feasible and beneficial.

1. INTRODUCTION

In the conventional methanol synthesis process, synthesis gas (CO_2, CO, and H_2) produced from natural gas in the reformer section is converted to methanol in a tubular packed-bed reactor. A schematic diagram of a conventional methanol synthesis reactor is shown in Figure 1a. The catalyst is packed in vertical tubes and surrounded by the boiling water. The methanol synthesis reactions are carried out over a commercial CuO/ZnO/Al_2O_3 catalyst. The heat of exothermic reactions is transferred to the boiling water and steam is produced.

The factors that affect the production rate in an industrial methanol reactor are parameters such as thermodynamic equilibrium limitations and catalyst deactivation. Two zones could be distinguished in the methanol synthesis reactor with imprecise transition point. The first zone starts from the reactor entrance and continues to a point where the conversion approaches equilibrium. In this zone, the kinetics control the process, so increasing the temperature improves the rate of reaction, which leads to more methanol production. Later, control of the process switches to equilibrium and, as the temperature increases, the deteriorating effects of equilibrium conversion emerge and decrease methanol production.[1,2] Therefore, two of the important key issues in methanol reactor configurations are implementing a higher temperature in the first parts of the reactor, for a higher reaction rate, and then reducing the temperature gradually at the end parts of the reactor, to increase the thermodynamic equilibrium conversion.

Recently, a steady-state thermally coupled reactor system—a novel recuperative coupling configuration for methanol synthesis and cyclohexane dehydrogenation—was developed by Khademi et al.[3] This reactor configuration permits a high temperature in the first part of the reactor and a low temperature in the second part. In this reactor, the catalytic dehydrogenation reaction of cyclohexane to benzene in the shell side is used instead of the cooler water in the conventional methanol synthesis reactor. Figure 1b shows a schematic diagram of thermally coupled reactor configuration. It consists of a shell compartment surrounding tube compartments. The catalytic dehydrogenation of cyclohexane to benzene is assumed to occur in the shell, whereas methanol synthesis occurs inside the tube, with a fixed bed of different catalysts on both sides. Heat is transferred continuously from the exothermic reaction to the endothermic reaction.

The clear advantages of this integrated catalytic reactor in comparison to conventional methanol synthesis reactor include (i) achieving a multiple reactants−multiple products configuration; (ii) improving the methanol yield by 3.1% under optimal conditions;[3] (iii) decreasing the exit temperature of the exothermic side to 505 K results in an increase in the thermodynamic equilibrium (exit temperature of conventional reactor is 525 K);[3] (iv) decreasing the average temperature of the endothermic side to 500 K (the temperature of cooler water in the conventional reactor is constant, 530 K);[3] (v) benzene is also produced as an additional valuable product; (vi) making the process more efficient and compact, resulting in large savings in the operational and capital costs; and (vii) the possibility of achieving a higher degree of in situ energy integration between the coupled endothermic dehydrogenation reaction and the exothermic synthesis reactions. It should be also mentioned that these recuperative coupling reactors have some disadvantages, such as (i) difference in the catalyst life of two beds, (ii) difficulty of replacement or recharge of the deactivated catalyst in the shell side, (iii) decreasing the number of degrees of freedom, and (iv) making the process significantly harder to operate (which can be overcome using advanced adaptive control).

Received: May 31, 2011
Accepted: September 15, 2011
Revised: August 11, 2011
Published: September 15, 2011

dx.doi.org/10.1021/ie201090b | *Ind. Eng. Chem. Res.* 2011, 50, 12092–12102

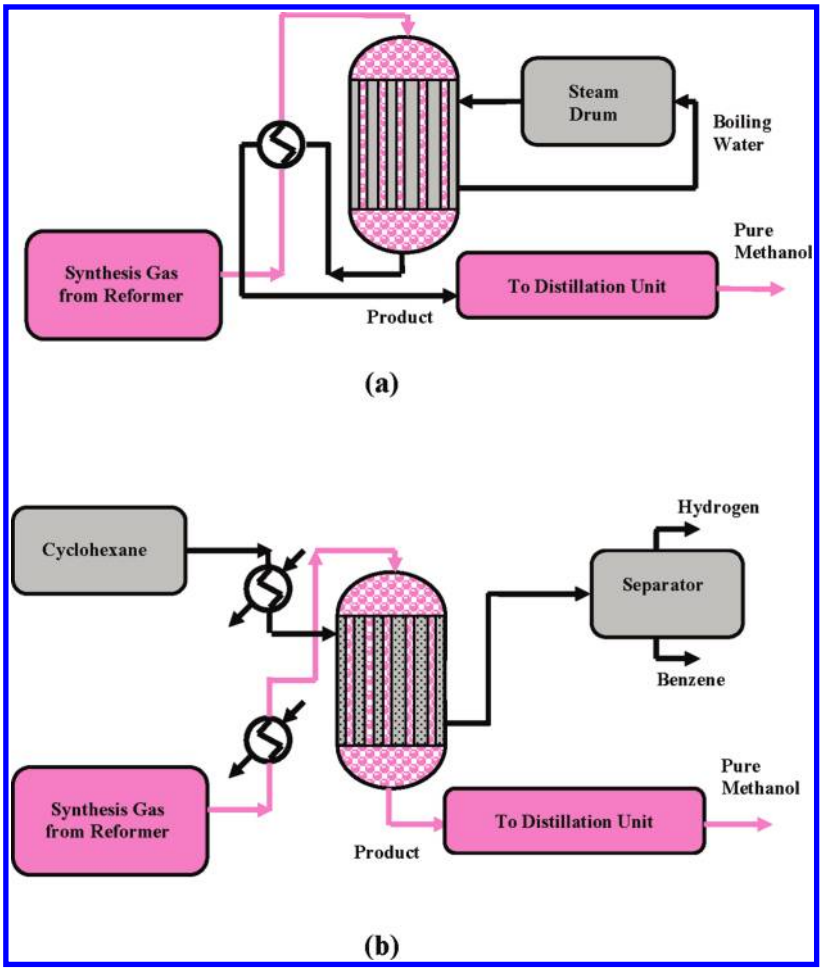

Figure 1. Schematic diagram of (a) a conventional methanol synthesis reactor and (b) a thermally coupled reactor configuration.

Also, Khademi et al.[4] developed a distributed mathematical model for the membrane thermally coupled reactor that is composed of three sides—exothermic, endothermic, and permeation sides—for methanol synthesis and cyclohexane dehydrogenation. The effect of various key operating variables on the performance of the reactor is numerically investigated under steady-state conditions. Therefore, using the optimal operating conditions can increase the production rate and reduce the operating costs; Khademi et al.[5] optimized the membrane thermally coupled reactor using a differential evolution method. The inlet temperature of all sides, initial molar flow rate of the exothermic and endothermic sides, and the inlet pressure of the exothermic side have been considered as decision variables to reach the maximum mole fraction of methanol, benzene, and hydrogen in the permeation side.

Based on the previous studies,[3−5] coupling of methanol synthesis and cyclohexane dehydrogenation reactions may enable both the concentration and temperature profiles along the reactor to be manipulated, shifting the conversion of thermodynamically limited reactions to higher values, and efficiently using the heat liberated by an exothermic reaction to provide the endothermic heat requirements of the other reaction.

The dynamic simulation of methanol synthesis processes, in particular, has a wide range of applications including the start-up and shut-down investigations, system identification, safety, control, optimization, and transient behavior and operability studies. The dynamic simulation is preferred to steady-state simulations in operability studies, since the former provides a realistic description of the transient states of the reactor, because of the fact that the numerical solution strategies employed in dynamic models are more robust than the solution of a typical steady-state model. Thus, it allows for safe and trustworthy studies of the control and optimization of the reactor.[6] Much research has been performed on dynamic modeling and optimization of the methanol synthesis reactor.[7−10] In this work, a dynamic heterogeneous model for the novel thermally coupled reactor—containing methanol synthesis reactions and cyclohexane dehydrogenation—was developed to identify the issue posed by the transient operation, including the potential for reactor extinction under normal operating circumstances or in the presence of frequently encountered disturbances. Also, the transient behavior during the start-up period of the reactor is investigated.

The paper is organized as follows: reactions scheme and kinetics are shown in Section 2. Mathematical model and numerical solution are explained in sections 3 and 4, respectively, followed by results and discussion in section 5. Conclusions are drawn in section 6.

2. REACTION SCHEME AND KINETICS

2.1. Methanol Synthesis. In the methanol synthesis, three overall reactions are possible: the hydrogenation of carbon

Table 1. Reaction Rate Constants, Adsorption Equilibrium Constants, and Reaction Equilibrium Constants for Methanol Synthesis and Dehydrogenation of Cyclohexane Reactions

definition	equation
Methanol synthesis reaction[a]	
reaction rate for CO hydrogenation	$r_1 = \frac{k_1 K_{CO}[f_{CO} f_{H_2}^{3/2} - f_{CH_3OH}/f_{H_2}^{1/2} K_{P1}]}{(1 + K_{CO} f_{CO} + K_{CO_2} f_{CO_2})[f_{H_2}^{1/2} + (K_{H_2O}/K_{H_2}^{1/2}) f_{H_2O}]}$
reaction rate of CO_2 hydrogenation	$r_2 = \frac{k_2 K_{CO_2}[f_{CO_2} f_{H_2}^{3/2} - f_{CH_3OH} f_{H_2O}/f_{H_2}^{3/2} K_{P2}]}{(1 + K_{CO} f_{CO} + K_{CO_2} f_{CO_2})[f_{H_2}^{1/2} + (K_{H_2O}/K_{H_2}^{1/2}) f_{H_2O}]}$
reaction rate for reversed water-gas shift reaction	$r_3 = \frac{k_3 K_{CO_2}[f_{CO_2} f_{H_2} - f_{H_2O} f_{CO}/K_{P3}]}{(1 + K_{CO} f_{CO} + K_{CO_2} f_{CO_2})[f_{H_2}^{1/2} + (K_{H_2O}/K_{H_2}^{1/2}) f_{H_2O}]}$
reactions rate constants	
k_1	$k_1 = 4.89 \times 10^7 \exp\left(\frac{-63000}{RT}\right)$
k_2	$k_2 = 1.09 \times 10^5 \exp\left(\frac{-87500}{RT}\right)$
k_3	$k_3 = 9.64 \times 10^6 \exp\left(\frac{-152900}{RT}\right)$
adsorption equilibrium constants	$K_{CO} = 2.16 \times 10^{-5} \exp\left(\frac{46800}{RT}\right)$
	$K_{CO_2} = 7.05 \times 10^{-7} \exp\left(\frac{61700}{RT}\right)$
	$\frac{K_{H_2O}}{K_{H_2}^{1/2}} = 6.37 \times 10^{-9} \exp\left(\frac{84000}{RT}\right)$
reaction equilibrium constants	$\log(K_{P1}) = \frac{5139}{T} - 12.621$
	$\log(K_{P2}) = \frac{3066}{T} - 10.592$
	$\log(K_{P3}) = -\frac{2073}{T} + 2.029$
Cyclohexane dehydrogenation reaction[b]	
reaction rate	$r_4 = \frac{-k(K_P P_C/P_{H_2}^3 - P_B)}{1 + (K_B K_P P_C/P_{H_2}^3)}$
reaction rate constant	$k = 0.221 \exp\left(-\frac{4270}{T}\right)$
benzene adsorption equilibrium constant	$K_B = 2.03 \times 10^{-10} \exp\left(\frac{6270}{T}\right)$
reaction equilibrium constant	$K_P = 4.89 \times 10^{35} \exp\left(\frac{3190}{T}\right)$

[a] Data taken from Graaf et al.[11] [b] Data taken from Itoh.[14]

monoxide, the hydrogenation of carbon dioxide, and the reverse water-gas shift reaction, which are as follows:

$$CO + 2H_2 \leftrightarrow CH_3OH \qquad \Delta H_{298} = -90.55 \text{ kJ/mol} \qquad (1)$$

$$CO_2 + 3H_2 \leftrightarrow CH_3OH + H_2O \qquad \Delta H_{298} = -49.43 \text{ kJ/mol} \qquad (2)$$

$$CO_2 + H_2 \leftrightarrow CO + H_2O \qquad \Delta H_{298} = +41.12 \text{ kJ/mol} \qquad (3)$$

Reactions 1−3 are not independent: one is a linear combination of the other ones. In the current work, the rate expressions have been selected from Graaf et al.[11] The rate equations, combined with the equilibrium rate constants,[12] provide enough information about the kinetics of methanol synthesis. The temperature and pressure of the reaction are 495−535 K and 5−8 MPa, respectively.[5]

2.2. Dehydrogenation of Cyclohexane. The endothermic reaction is the dehydrogenation of cyclohexane to benzene. The temperature of this reaction is in the range of 423−523 K, and the total pressure in the reactor is maintained at 101.3 kPa. The catalyst for this reaction is Pt/Al_2O_3.[13] The reaction scheme for the dehydrogenation of cyclohexane to benzene is as follows:

$$C_6H_{12} \leftrightarrow C_6H_6 + 3H_2 \qquad \Delta H_{298} = +206.2 \text{ kJ/mol} \qquad (4)$$

The reaction rates, the reaction rate constants, the adsorption equilibrium constants, and the reaction equilibrium constants for both reactions are tabulated in Table 1.

3. MATHEMATICAL MODEL

Although an experimental proof-of-concept is needed to establish the validity and safe operation of the novel reactor, rigorous mathematical models are excellent tools for the exploration of the basic characteristics of such novel configurations. Such an exploration can achieve considerable savings in money and time during the expensive stage of pilot-plant development. The continuous development of the model, in conjunction with the pilot-plant optimal utilization, can also achieve considerable benefits on the road toward the successful commercialization of such efficient novel configurations.

Figure 2 shows a schematic diagram of the co-current mode for a thermally coupled reactor configuration. A dynamic one-dimensional heterogeneous model, which is a conventional model for a catalytic reactor with heat- and mass-transfer resistances, has been developed for this reactor in order to determine the concentration and temperature distributions inside the reactor. In this model, the following assumptions are used:

- The gas mixture is an ideal gas in both catalytic reactor sides.
- A two-dimensional steady-state simulation of a conventional methanol synthesis reactor shows that the properties of the reactor are not varying, relative to the radius of the catalyst tube.[1] Also, to minimize radial temperature gradients, radial aspect ratios (d_p/R_t) in the range of $^1/_8$−$^1/_5$ is used.[15] Therefore, the radial variations of concentration and temperature within both beds of the reactor are negligible, because of the small radius, relative to the length of the tube (one-dimensional model).
- The axial diffusion of mass and heat is significantly lower than the gas bulk movement in both sides; also, since $L/d_p > 30$, axial dispersion is neglected.[16]
- Bed porosity in the axial and radial directions is constant.
- Since the bed voidage at the reactor wall is higher than the average, the velocity profile in the bed is not uniform. These deviations from a flat profile can be neglected if $D_i/d_p > 15$.[17] Therefore, plug flow is employed in both the endothermic and exothermic sides.
- The chemical reactions are assumed to take place only in the catalyst particles and homogeneous reactions are neglected.
- Heat loss to the surroundings is neglected.
- A uniform temperature is assumed inside the particles in both catalytic sides, due to a Biot number (Bi) of <0.1.

To obtain the mole balance equation and the energy balance equation, a differential element along the axial direction inside the reactor was considered (see Figure 2). The balances typically account for accumulation, convection, transport to the solid-phase, and the reaction.

3.1. Solid Phase. The mass and energy balances for the solid phase are expressed by

$$(1 - \varepsilon_B) c_j \frac{\partial y_{i,j}^s}{\partial t} = a_v c_j k_{gi,j} (y_{i,j}^g - y_{i,j}^s) + \eta r_{i,j} \rho_b \qquad (5)$$

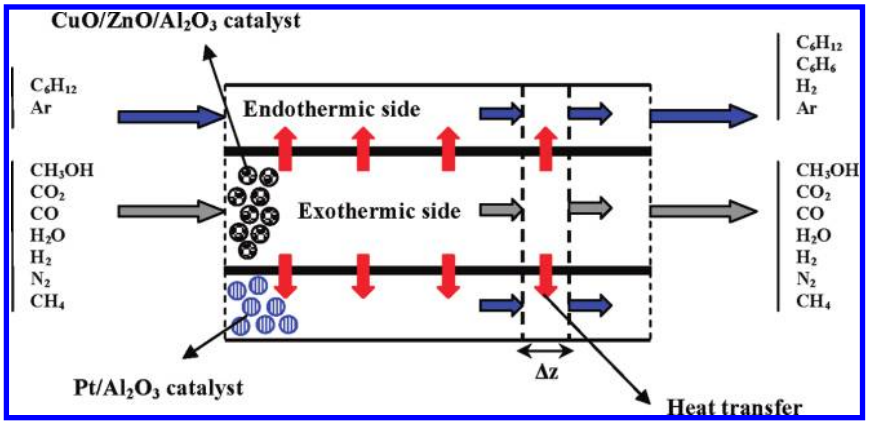

Figure 2. Schematic diagram of the co-current mode for a thermally coupled reactor configuration.

$$\rho_b C_{pj}^s \frac{\partial T_j^s}{\partial t} = a_v h_f (T_j^g - T_j^s) + \rho_b \sum_{k=1}^{N_k} \eta r_{i,j} (-\Delta H_{f,i}) \quad (6)$$

where $y_{i,j}^s$ and T_j^s are the solid-phase mole fraction and temperature in the j side of reactor, respectively, and η is the effectiveness factor (the ratio of the actual reaction rate to the rate of reaction at the catalyst surface), which is obtained from dusty gas model calculations. Details of the dusty gas model are presented by Khademi et al.[3]

3.2. Fluid Phase. The following mass and energy balances equations are written for the fluid phase:

$$\varepsilon_B c_j \frac{\partial y_{i,j}^g}{\partial t} = -\frac{1}{A_c} \frac{\partial (F_j y_{i,j}^g)}{\partial z} + a_v c_j k_{gi,j} (y_{i,j}^s - y_{i,j}^g) \quad (7)$$

$$\varepsilon_B c_j C_{pj}^g \frac{\partial T_j^g}{\partial t} = -\frac{1}{A_c} C_{pj}^g \frac{\partial (F_j T_j^g)}{\partial z} + a_v h_f (T_j^s - T_j^g) \pm \left(\frac{\pi D_i}{A_c}\right) U (T_2^g - T_1^g) \quad (8)$$

where $y_{i,j}^g$ and T_j^g are the fluid-phase mole fraction and temperature in the j side of the reactor, respectively. In eq 8, the positive sign is used for the exothermic side and the negative sign is used for the endothermic side.

3.3. Pressure Drop. The Ergun momentum balance equation is used to give the pressure drop along the reactor:

$$\frac{dP}{dz} = 150 \left[\frac{(1-\varepsilon)^2 \mu u_g}{\varepsilon^3 d_p^2}\right] + 1.75 \left[\frac{(1-\varepsilon) u_g^2 \rho}{\varepsilon^3 d_p}\right] \quad (9)$$

where the pressure drop is given in pascals.

3.4. Boundary and Initial Conditions. The boundary and initial conditions, applied to solve the model for the cases of "dynamic analysis" and "start-up analysis", are discussed in this section.

3.4.1. Dynamic Analysis. At the entrance of the reactor, the inlet temperature, the inlet pressure, and the inlet gas compositions of the reactant gas in the both sides are known. Therefore, the following boundary conditions are applied:

$$z = 0,\ y_{i,j}^g = y_{i0,j}^g,\ T^g = T_0^g,\ P^g = P_0^g \quad (10)$$

where $y_{i0,j}^g$, T_0^g, and P_0^g are the fluid-phase mole fraction, temperature, and pressure at the entrance of the j side of the reactor, respectively.

While the initial conditions are

$$t = 0,\ y_{i,j}^g = y_{i,j}^{g,ss},\ y_{i,j}^s = y_{i,j}^{s,ss},\ T_j^g = T_j^{g,ss},\ T_j^s = T_j^{s,ss} \quad (11)$$

where $y_{i,j}^{g,ss}$ and $y_{i,j}^{g,ss}$ are the steady-state profiles of the mole fraction and $T_j^{g,ss}$ and $T_j^{s,ss}$ are the steady-state profiles of temperature along the reactor. The values of $y_{i,j}^{g,ss}$, $y_{i,j}^{g,ss}$, $T_j^{g,ss}$ and $T_j^{s,ss}$ are determined from a steady-state simulation.

3.4.2. Start-Up Analysis. The boundary conditions for the "start-up analysis" case are the same as those used for the "dynamic analysis" case. At low temperature, almost no reaction occurs, because of the temperature-sensitive reaction rate. Therefore, the initial temperature for the both catalyst beds was set to uniform temperature and equal to the incoming feed temperature (T_0^g = 503 K). The value of zero for mole fraction of components results in infinite reaction rates. Therefore, the initial mole fraction of components in the both sides was selected to be 10^{-7} at the initial time of startup.

$$t = 0,\ y_{i,j}^g = 10^{-7},\ y_{i,j}^s = 10^{-7},\ T_j^g = T_0^g,\ T_j^s = T_0^g \quad (12)$$

3.5. Auxiliary Correlations. To complete the simulation, auxiliary correlations should be added to the model. In the heterogeneous model, because of transfer phenomena, the correlations of estimation of heat and mass transfer between two phases and estimation of physical properties of chemical species and the overall heat-transfer coefficient between two sides should be considered. The correlations used for physical properties, and the mass- and heat-transfer coefficient, are summarized in Table 2. For the heat-transfer coefficient between the bulk gas phase and the solid phase (h_f) in the exothermic and endothermic side, the heat-transfer coefficient between the gas phase and the reactor wall is applicable.

4. NUMERICAL SOLUTION

The governing equations of the model form a system of coupled equations comprised of algebraic equations, partial differential equations (PDEs), and ordinary differential equations (ODEs). The system of equations is solved using a two-stage approach, consisting of a steady-state identification stage followed by a dynamic solution stage. The steady-state and dynamic models are used to identify the dynamic response of

Table 2. Physical Properties and Mass- and Heat-Transfer Correlations

parameter	equation	reference
component heat capacity	$C_p = a + bT + cT^2 + dT^3$	Reid et al.[18]
mixture heat capacity	based on local compositions	
viscosity of reaction mixtures	based on local compositions	
mixture thermal conductivity		Lindsay and Bromley[19]
mass-transfer coefficient between gas and solid phases	$k_{gi} = 1.17Re^{-0.42}Sc_i^{-0.67}u_g \times 10^3$	Cussler[20]
	$Re = \frac{2R_p u_g \rho}{\mu}$ $Sc_i = \frac{\mu}{\rho D_{im} \times 10^{-4}}$	
	$D_{im} = \frac{1 - y_i}{\sum_{i=j} \frac{y_i}{D_{ij}}}$	Wilke[21]
	$D_{ij} = \frac{10^{-7} T^{3/2} \sqrt{1/M_i + 1/M_j}}{P(v_{ci}^{1/3} + v_{cj}^{1/3})^2}$	Reid et al.[18]
overall heat-transfer coefficient	$\frac{1}{U} = \frac{1}{h_i} + \frac{A_i \ln(D_o/D_i)}{2\pi L K_w} + \frac{A_i}{A_o}\frac{1}{h_o}$	
heat-transfer coefficient between the gas phase and the reactor wall	$\frac{h}{C_p \rho \mu}\left(\frac{C_p \mu}{K}\right)^{2/3} = \frac{0.458}{\varepsilon_B}\left(\frac{\rho u d_p}{\mu}\right)^{-0.407}$	Smith[22]

reactor to apply one step change in the reactor inlet, and just dynamic model is used to analyze start-up conditions.

4.1. Steady-State Identification. Identifying the steady-state condition of the thermally coupled reactor, in principle, is simply a matter of determining the concentration and temperature profiles along the reactor axis at time zero. This is accomplished by setting all time derivatives of the states equal to zero. In this way, the initial conditions for temperature and concentration are determined for dynamic simulation.

After rewriting the model equations under steady-state conditions, a set of differential algebraic equations (DAEs) is obtained. To solve this set of equations, backward finite difference approximation is applied here. Doing this, the DAEs change to a nonlinear algebraic set of equations. The reactor is then divided into 40 separate sections and the Gauss−Newton method is used to solve the nonlinear algebraic equations in each section. The result of the steady-state simulation is used as initial conditions for time integration of dynamic-state equations in each node through the reactor.

4.2. Solution of Dynamic Model. The set of dynamic equations consists of simultaneous ODEs and PDEs, because of the conservation rules, as well as the algebraic equations, because of the auxiliary correlations, kinetics, and thermodynamics of the reaction system. After discretization of the PDEs on the nodes of a one-dimensional mesh in the axial direction, a system of ODEs is obtained for each node. The time step used in this work (Δt = 0.01 s) must be shorter than residence time scales of the reacting flows inside the both channels. One characteristic feature of the system is its stiffness. The spatial discretization causes stiffness, because of local variations in the rate of kinetic and transfer processes. Initially, we had tried to solve the equations using the Runge−Kutta method of different orders, as well as Euler and modified Euler methods; however, because of the divergence of the numerical solution, the use of these methods was abandoned. Therefore, a modified second-order Rosenbrock formula, which is an iterative multistage procedure and is well-suited for the system of stiff equations,[23] was used and the system of model equations was conveniently converged.

5. RESULTS AND DISCUSSIONS

In this section, various dynamic behaviors observed in the co-current thermally coupled reactor is analyzed and the predicted methanol and benzene yields, cyclohexane conversion, and temperature profiles are presented. The performance of the thermally coupled reactor is analyzed, using different operating variables, for methanol and benzene yields and cyclohexane conversion as follows:

$$\text{methanol yield} = \frac{F_{CH_3OH,\,out}}{F_{CO,\,in} + F_{CO_2,\,in}} \tag{13}$$

$$\text{benzene yield} = \frac{F_{C_6H_6,\,out}}{F_{C_6H_{12},\,in}} \tag{14}$$

$$\text{cyclohexane conversion} = \frac{F_{C_6H_{12},\,in} - F_{C_6H_{12},\,out}}{F_{C_6H_{12},\,in}} \tag{15}$$

The operating conditions used for both sides of the reactor are given in Table 3. Operating conditions for the methanol synthesis side are similar to those used by Rezaie et al.[26] The inlet composition of the methanol synthesis reaction is typical of the industrial methanol synthesis process. It corresponds to a hydrogen:carbon-dioxide ratio of 7, having small amounts of CH_3OH, CO, and H_2O, together with inert gases of CH_4 and N_2. On the endothermic side, the inlet mole fraction of cyclohexane that is diluted with argon is the same as that presented by Jeong et al.[24] Thus, these operating conditions are used to investigate the situation when the cyclohexane dehydrogenation is used to consume the heat generated from the methanol synthesis and to cool it down, resulting in a higher temperature in the first parts of the exothermic side for higher kinetics constants and then reduced temperature gradually in the end parts of reactor for increasing thermodynamics equilibrium, which is similar to the temperature profile along a tube filled with catalyst within a methanol conventional reactor. This allows comparison of the methanol synthesis process in the coupled reactor with conventional methanol reactor (CMR) for similar thermal behavior.

Table 3. Operating Conditions for Methanol Synthesis Process (Exothermic Side) and Dehydrogenation of Cyclohexane to Benzene (Endothermic Side)

parameter	value
Exothermic Side	
Gas phase	
feed composition (mole fraction)	
CH_3OH	0.005
CO_2	0.094
CO	0.046
H_2O	0.0004
H_2	0.659
N_2	0.093
CH_4	0.1026
total molar flow rate (mol s^{-1})	0.64
inlet temperature (K)	503
inlet pressure (bar)	76.98
Catalyst particle	
density (kg m^{-3})	1770
particle diameter (m)	5.47×10^{-3}
heat capacity (kJ kg^{-1} K^{-1})	5.0
thermal conductivity (W m^{-1} K^{-1})	0.004
specific surface area (m^2 m^{-3})	626.98
ratio of void fraction to tortuosity of catalyst particle	0.123
Length of reactor (m)	7.022
Bed void fraction	0.39
Density of catalyst bed (kg m^{-3})	1140
Inner diameter of tube (m)	3.8×10^{-2}
Outer diameter of tube (m)	4.2×10^{-2}
Wall thermal conductivity (W m^{-1} K^{-1})	48
Endothermic Side	
Gas phase	
feed composition[a] (mole fraction)	
C_6H_{12}	0.1
C_6H_6	0.0
H_2	0.0
Ar	0.9
total molar flow rate (mol s^{-1})	0.1
inlet temperature (K)	503
inlet pressure[a] (Pa)	1.013×10^5
particle diameter[b] (m)	3.55×10^{-3}
Bed void fraction	0.39
Inner diameter of shell (m)	6×10^{-2}

[a] Data taken from Jeong et al.[24] [b] Data taken from Koukou et al.[25]

The simulation results of the reactor in the endothermic side are not compared with any reference case.

5.1. Steady-State Model Validation. Validation of the steady-state model was carried out via a comparison of the model results with the plant data[27] (from Shiraz Petrochemical Complex) at time zero for conventional methanol reactor under the design specifications and input data tabulated in Table 3 at the "exothermic side" section. The model results and the corresponding observed data of the plant are presented in Table 4. It was observed that, the steady-state model performed satisfactorily well under industrial conditions and a good agreement between plant data and simulation data existed. The comparison between the results of novel thermally coupled and conventional methanol reactors at the steady-state condition is presented by Khademi et al.[4]

Table 4. Comparison between Steady-State Simulation and Plant Data for Conventional Methanol Synthesis Reactor

		Reactor Outlet	
	reactor inlet	plant	calc.
composition (mol %)			
CO_2	3.45	2.18	2.43
CO	4.66	1.44	1.52
H_2	79.55	75.71	76.54
CH_4	11.72	12.98	12.96
N_2	0.032	0.16	0.035
H_2O	0.08	1.74	1.47
CH_3OH	0.032	5.49	5.05
feed flow rate (mol s^{-1})	0.565	0.510	0.511
temperature (K)	503	528	524.1
pressure (bar)	61.83	61.16	61.59

Table 5. Comparison between the Calculated Methanol Production Rate and the Daily Observed Plant Data for a Conventional Methanol Synthesis Reactor

time (day)	plant (tonnes/day)	calc. (tonnes/day)	error percent
0	295.0	308.80	2.93
100	296.5	297.03	0.18
200	302.6	289.10	−4.46
300	284.3	283.09	−0.44
400	277.9	278.19	0.10
500	278.2	274.03	−1.50
600	253.0	270.41	6.88
700	274.0	267.19	−2.48
800	268.1	264.30	−1.65
900	275.5	261.67	−5.02
1000	274.6	259.25	−5.58
1100	262.9	257.02	−2.24
1200	255.2	255.18	−0.05

5.2. Dynamic Model Validation. In order to verify the goodness of the dynamic model, simulation results have been compared with the historical process data[27] (from Shiraz Petrochemical Complex) for a conventional methanol reactor in the presence of catalyst deactivation. The predicted results of production rate and the corresponding observed data of the plant are presented in Table 5. It was observed that, the model performed satisfactorily well under industrial conditions, and good agreement was observed between daily observed plant data and simulation data.

5.3. Start-up Analysis. Dynamic simulation is carried out during the start-up period to address the vital issues, such as the exothermic and endothermic side temperatures and methanol and benzene yields, as a function of time and length of reactor. In Figure 3, dynamic variation of the exothermic side temperature along the reactor length has been illustrated in a three-dimensional diagram at the start-up phase. Figure 4 represents time

variations of methanol and benzene yields and exothermic and endothermic side temperatures at dimensionless lengths of 0.2, 0.4, 0.6, 0.8, and 1.0. The distributions of temperatures and methanol and benzene yields move forward during the initial times of the start-up period. As it can be seen in this figure, the residence time of the reacting flows inside the exothermic and endothermic sides are ~20 and ~1.3 s, respectively. The residence time of the reacting flows inside the endothermic side is lower than that inside the exothermic side. Therefore, the required heat for cyclohexane dehydrogenation reaction is supplied from the sensible heat of the reacting flow and the temperature decreases to 450 K after 1.3 s at the reactor exit (see Figure 4d). At the initial times of start-up period (<20 s), the reaction rate of methanol synthesis is low and the transferred heat from the solid wall becomes higher than the generated one; therefore, a temperature reduction is observed at this time domain in Figure 4c.

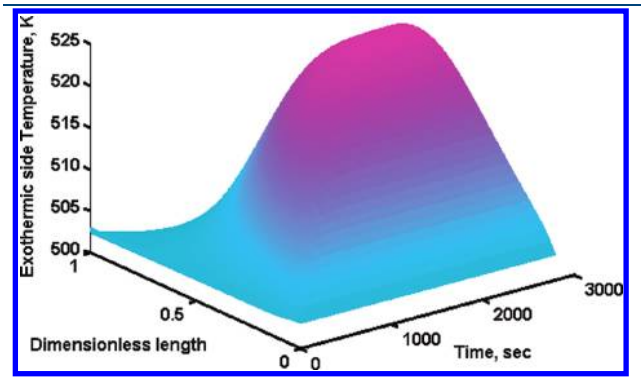

Figure 3. Dynamic variation of the exothermic side temperature along the reactor length.

The system approaches the steady-state condition after ~2750 s. At the steady state, the methanol and benzene yields increase along the reactor length. After ~2750 s, the methanol and benzene yields reach 0.37 and 0.79, respectively, at the reactor exit (see Figures 4a and 4b).

At steady state and along the exothermic side of the reactor, the temperature increases smoothly and a hot spot (523 K) develops at dimensionless length $z/L = 0.7$, as demonstrated in Figure 4c, and then decreases to 515 K. In the first half of the reactor, the methanol reaction proceeds at a higher rate than dehydrogenation; as a result, more heat is produced by the exothermic reaction than consumed by the endothermic one. The excess heat increases the temperature of the exothermic side in the first half of the reactor at the steady state.

At steady state and the entrance of the dehydrogenation side, the temperature decreases rapidly and a cold spot (495 K) forms at the axial dimensionless position of $z/L = 0.07$, because of relatively low reaction rate, and then the temperature increases (see Figure 4d). After a certain position along the reactor (dimensionless length $z/L = 0.7$ in Figure 4d), the heat transferred from the solid wall becomes lower than the consumed one,

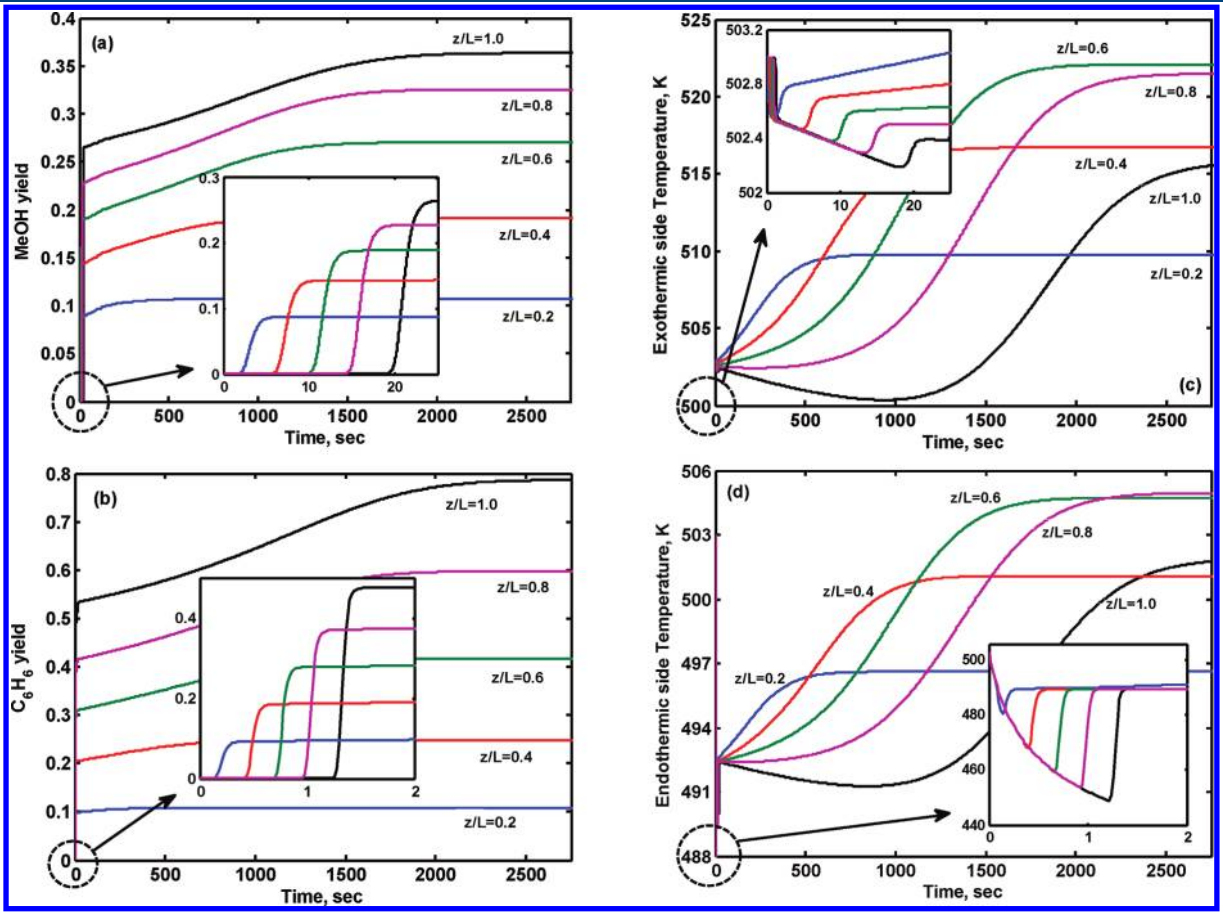

Figure 4. time variations of (a) methanol yield, (b) benzene yield, (c) exothermic side temperature, and (d) endothermic side temperature at dimensionless lengths of 0.2, 0.4, 0.6, 0.8, and 1.0.

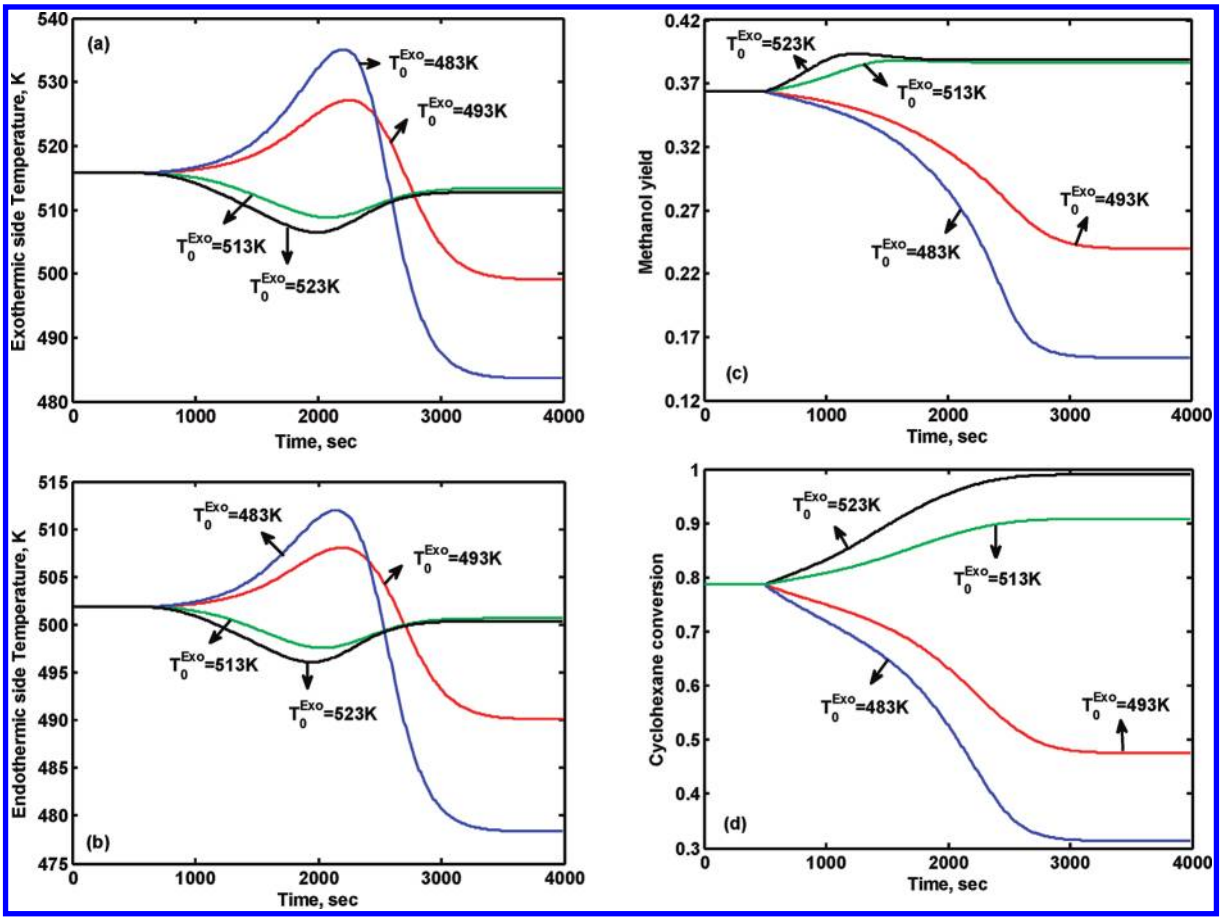

Figure 5. Transient profiles of (a) exothermic side temperature, (b) endothermic side temperature, (c) methanol yield, and (d) cyclohexane conversion at the reactor exit for two increases in the inlet temperature on the exothermic side (from 503 K to 513 K and 523 K) and for two decreases (from 503 K to 493 K and 483 K).

which coincides with the development of a hot spot (507 K). Note that, in the endothermic side at steady state, the outlet temperature (at $z/L = 1.0$) is the same as the inlet temperature (502 K).

5.4. Dynamic Analysis. To investigate the influence of disturbances on the dynamic behavior of this novel reactor, the feed temperature and molar flow rate have been considered as the main probable effective loads of the system. In this section, the dynamic behaviors observed in the reactor, because of variations of inputs, are analyzed and the estimated methanol and benzene yields and temperature profiles of both sides are presented. The dynamic simulations of the autothermal reactor were initially carried out at the reactor exit. The feed temperature of the exothermic side is the most important parameter in this novel reactor subsequently; a variation in the initial temperature was introduced in the exothermic side at 500 s. Figure 5 shows the transient profiles of the representative reactor variables at the reactor exit, as the gas inlet temperature of the exothermic side is decreased from 503 K to 493 K and 483 K and increased from 503 K to 513 K and 523 K. Initial molar flow rates of the gases in both sides and the feed temperature of the endothermic side are kept constant at their base values of, respectively, 0.64, 0.1 mol s^{-1}, and 503 K, respectively. Such a disturbance could occur, e.g., in the case of a faulty or decalibrated thermocouple in the preheater of the reactor. As can be seen in Figure 5c and 5d, decreases of 20 K in the feed temperature lead to decreases the methanol yield and cyclohexane conversion to 0.15 and 32%, respectively. This disturbance leads to the extinction of the reactor after >3500 s. This phenomenon can be explained, the decreased reaction rates and rate of heat generation due to reduction of the reactor temperature notwithstanding, by considering that lower inlet temperatures lead to lower temperatures in the gas phase over the entire length of the reactor. By way of consequence, this process continues until a relative extinction is reached at 3500 s.

Increases of 10 K and 20 K in the feed temperature of the exothermic side (e.g., T_0^{Exo} = 513 K and 523 K) have no significant effect on the methanol yield and temperature profiles of both sides at the reactor exit. Notice the highly nonlinear behavior; this disturbance results in a new steady state close to the nominal operating point (see Figures 5a−c). On the other hand, a larger rise in feed temperature (T_0^{Exo} = 523 K) drives the cyclohexane conversion far away from the nominal steady state and, the value of this parameter reaches to 99% (see Figure 5d).

Applying step changes of ±10 K and ±20 K in the inlet temperature of the endothermic side have no significant effect on the variations of the transient methanol yield (±0.01) and temperature profiles (±2 K) of both sides at the reactor exit. These disturbances (+20, +10, −10, and −20 K) respectively, lead to new steady-state cyclohexane conversions (86%, 82.5%, 74.5%, and 70% after >3500 s).

Figure 6 presents the response of the reactor outlet temperature for the both sides in the ±10% and ±20% cases increasing/

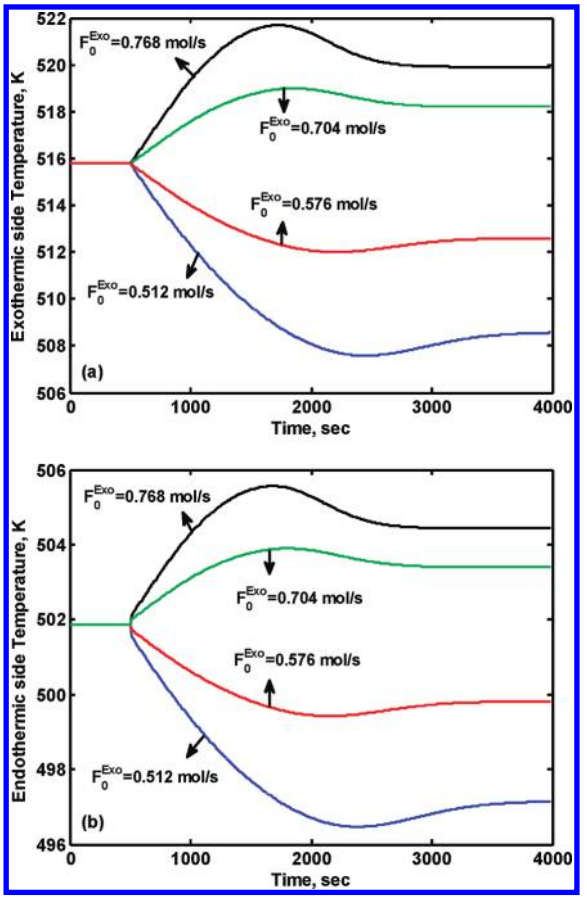

Figure 6. Transient profiles of (a) exothermic side temperature and (b) endothermic side temperature at the reactor exit for two increases in initial molar flow rate of the exothermic side from 0.64 mol s^{-1} to 0.704 mol s^{-1} and 0.768 mol s^{-1} and for two decreases in that from 0.64 mol s^{-1} to 0.576 mol s^{-1} and 0.512 mol s^{-1}.

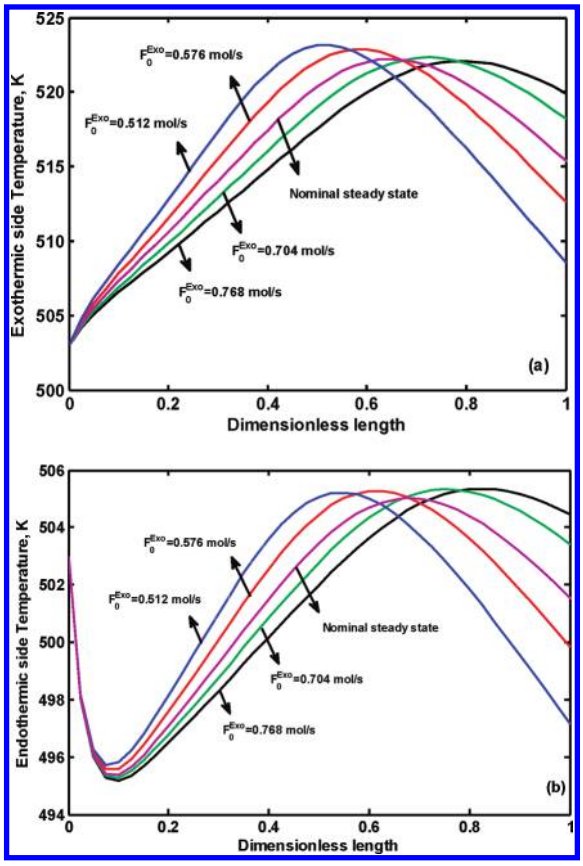

Figure 7. Steady-state spatial profiles of (a) exothermic side temperature and (b) endothermic side temperature at the nominal steady state (0.64 mol s^{-1}), for two increases in the initial molar flow rate of exothermic side from 0.64 mol s^{-1} to 0.704 mol s^{-1} and 0.768 mol s^{-1} and for two decreases in that from 0.64 mol s^{-1} to 0.576 mol s^{-1} and 0.512 mol s^{-1}.

decreasing in the initial molar flow rate of the gas in the exothermic side. The initial molar flow rate of the gas in the endothermic side is kept constant at its nominal value of 0.1 mol s^{-1}. As shown in this figure, increasing this disturbance from 0.704 mol s^{-1} to 0.768 mol s^{-1} leads to an increase in the new steady-state temperature in both sides, and decreasing this disturbance from 0.576 mol s^{-1} to 0.512 mol s^{-1} results in decreasing that at the reactor exit.

Figure 7 presents the reactor temperature profiles for F_0^{Exo} = 0.64 mol s^{-1} (nominal steady state), as well as for F_0^{Exo} = 0.512, 0.576, 0.704, and 0.768 mol s^{-1}. This figure illustrates the temperature shifting at the nominal peak position and the migration of the location of the temperature peak as the inlet velocity of the synthesis gas is varied. The strengthening of convective heat transport due to the higher velocity leads to coerce the wave-shaped spatial temperature distribution to shift to the right (toward the reactor exit) and ultimately forcing the heat wave to leave the reactor altogether. As it can be seen in Figure 7a, increasing the axial velocity of the gas in the exothermic side causes the migration of the wave profile toward the reactor outlet, as well as a decrease in this temperature at the point where the temperature "peak" is located at steady state. Similarly, decreasing the molar flow rate in the exothermic side leads to an increase in temperature at the nominal peak location and causes the temperature peak to shift to the left.

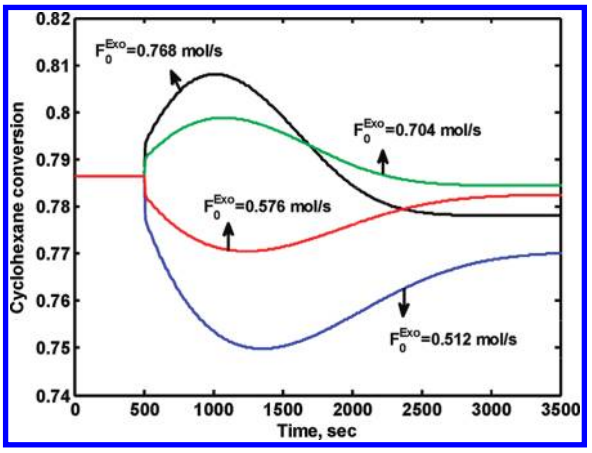

Figure 8. Transient profiles of cyclohexane conversion at the reactor exit for two increases in the initial molar flow rate on the exothermic side from 0.64 mol s^{-1} to 0.704 mol s^{-1} and 0.768 mol s^{-1} and for two decreases in that from 0.64 mol s^{-1} to 0.576 mol s^{-1} and 0.512 mol s^{-1}.

The temperature profile in the exothermic side affects the endothermic side temperature, and behavior similar to the trend in exothermic side temperature occurs on the endothermic side (see Figure 7b).

The transient response of cyclohexane conversion with four step changes in the initial molar flow rate of the exothermic side is shown in Figure 8. The cyclohexane conversion response at the reactor exit exhibits an initial fast transient that is followed by a slow evolution to a new steady state close to the nominal steady state (78.7%). Note that this disturbance can change the methanol yield slightly (±0.02) at the reactor exit during the time.

6. CONCLUSION

The methanol synthesis reaction, coupled with the dehydrogenation of cyclohexane to benzene by means of indirect heat transfer in a catalytic heat-exchanger reactor, was studied using a dynamic heterogeneous model. The developed computer code was shown to be able to describe the start-up and transient behavior of this coupled reactor in detail and led to a better understanding of this system. A base case was generated considering similar operating conditions to an industrial methanol reactor. The start-up operation of this novel thermally coupled reactor was accomplished over a period of ~2750 s. Dynamic simulation results for the co-current mode have been investigated to present the response of the reactor outlet temperature, methanol yield, and cyclohexane conversion in the cases of a step change in the initial molar flow rate and inlet temperature of both sides. Furthermore, the issues and challenges posed by the transient operation of this reactor were identified. It was shown that this autothermal reactor can exhibit highly nonlinear behavior, with the potential for reactor extinction at certain regions in the operating parameter range. The results indicate that the feed temperature of exothermic side is the major process disturbance that should be damped by the designed control system. It should be mentioned that this coupled reactor makes the process significantly harder to operate than a conventional methanol reactor, which can be overcome to this challenge using advanced adaptive control. The results indicated that methanol synthesis and cyclohexane dehydrogenation reactions in a heat-exchanger reactor could be feasible if the molar flow rates and inlet temperatures of the both sides can be properly controlled. In addition, the use of a feedback controlling system is under investigation by these coauthors.

AUTHOR INFORMATION

Corresponding Author

*Tel.: +98 711 2303071. Fax: +98 711 6287294. E-mail: rahimpor@shirazu.ac.ir.

NOMENCLATURE

a_v = specific surface area of catalyst pellet ($m^2\ m^{-3}$)
A_c = cross-sectional area of each tube (m^2)
A_i = inside area of inner tube (m^2)
A_o = outside area of inner tube (m^2)
c = total concentration (mol m^{-3})
C_p = specific heat of the gas at constant pressure (J mol^{-1})
d_p = particle diameter (m)
D_i = tube inside diameter (m)
D_{ij} = binary diffusion coefficient of component i in j ($m^2\ s^{-1}$)
D_{im} = diffusion coefficient of component i in the mixture ($m^2\ s^{-1}$)
D_o = tube outside diameter (m)
D_{sh} = shell inside diameter (m)
E_d = activation energy (J mol^{-1})
f_i = partial fugacity of component i (bar)
F = total molar flow rate (mol s^{-1})
G = mass velocity (kg $m^{-2}\ s^{-1}$)
h_f = gas−solid heat transfer coefficient (W $m^{-2}\ K^{-1}$)
h_i = heat-transfer coefficient between the fluid phase and the reactor wall on the exothermic side (W $m^{-2}\ K^{-1}$)
h_o = heat-transfer coefficient between the fluid phase and the reactor wall on the endothermic side (W $m^{-2}\ K^{-1}$)
$\Delta H_{f,i}$ = enthalpy of formation of component i (J mol^{-1})
k = rate constant of dehydrogenation reaction (mol $m^{-3}\ Pa^{-1}\ s^{-1}$)
k_1 = rate constant for the first rate equation of methanol synthesis reaction (mol $kg^{-1}\ s^{-1}\ bar^{-1/2}$)
k_2 = rate constant for the second rate equation of methanol synthesis reaction (mol $kg^{-1}\ s^{-1}\ bar^{-1/2}$)
k_3 = rate constant for the third rate equation of methanol synthesis reaction (mol $kg^{-1}\ s^{-1}\ bar^{-1/2}$)
k_g = mass-transfer coefficient for component i ($m\ s^{-1}$)
K = conductivity of fluid phase (W $m^{-1}\ K^{-1}$)
K_B = adsorption equilibrium constant for benzene (Pa^{-1})
K_d = deactivation constant of $CuO/ZnO/Al_2O_3$ catalyst (h^{-1})
K_i = adsorption equilibrium constant for component i in methanol synthesis reaction (bar^{-1})
K_p = equilibrium constant for the dehydrogenation reaction (Pa^3)
K_{p_i} = equilibrium constant based on the partial pressure for component i in methanol synthesis reaction
K_w = thermal conductivity of reactor wall (W $m^{-1}\ K^{-1}$)
L = reactor length (m)
M_i = molecular weight of component i (g mol^{-1})
N = number of components; $N = 6$ for methanol synthesis reaction, $N = 3$ for dehydrogenation reaction
P = total pressure for the exothermic side (bar) and the endothermic side (Pa)
P_i = partial pressure of component i (Pa)
r_1 = rate of reaction for the hydrogenation of CO (mol $kg^{-1}\ s^{-1}$)
r_2 = rate of reaction for the hydrogenation of CO_2 (mol $kg^{-1}\ s^{-1}$)
r_3 = rate of the reverse water-gas shift reaction (mol $kg^{-1}\ s^{-1}$)
r_4 = rate of reaction for the dehydrogenation of cyclohexane (mol $m^{-3}\ s^{-1}$)
r_i = reaction rate of component i for the exothermic reaction (mol $kg^{-1}\ s^{-1}$) and the endothermic reaction (mol $m^{-3}\ s^{-1}$)
R = universal gas constant (J $mol^{-1}\ K^{-1}$)
R_p = particle radius (m)
R_t = tube radius (m)
Re = Reynolds number
Sc_i = Schmidt number of component i
t = time (s)
T = temperature (K)
T_R = reference temperature (K)
u = superficial velocity of the fluid phase ($m\ s^{-1}$)
u_g = linear velocity of the fluid phase ($m\ s^{-1}$)
U = overall heat-transfer coefficient between the exothermic and endothermic sides (W $m^{-2}\ K^{-1}$)
v_{ci} = critical volume of component i ($cm^3\ mol^{-1}$)
y_i = mole fraction of component i (mol mol^{-1})
z = axial reactor coordinate (m)

Greek Letters

ε = void fraction
ε_B = void fraction of catalytic bed
μ = viscosity of fluid phase (kg $m^{-1}\ s^{-1}$)
ρ = density of fluid phase (kg m^{-3})

ρ_b = density of catalytic bed (kg m^{-3})
τ = tortuosity of catalyst

Superscripts

g = in bulk gas phase
s = at surface catalyst
ss = steady-state conditions
Endo = endothermic side
Exo = exothermic side

Subscripts

0 = inlet conditions
B = benzene
C = cyclohexane
i = chemical species
j = reactor side index; j = 1 for the exothermic side, j = 2 for the endothermic side
k = reaction number index

REFERENCES

(1) Jahanmiri, A.; Eslamloueyan, R. Optimal Temperature Profile in Methanol Synthesis Reactor. *Chem. Eng. Commun.* **2002**, *189*, 713–741.

(2) Aris, R. *The Optimal Design of Chemical Reactors*; Academic Press: New York, 1961.

(3) Khademi, M. H.; Setoodeh, P.; Jahanmiri, A.; Rahimpour, M. R. Optimization of methanol synthesis and cyclohexane dehydrogenation in a thermally coupled reactor using differential evolution (DE) method. *Int. J. Hydrogen Energy* **2009**, *34*, 6930–6944.

(4) Khademi, M. H.; Jahanmiri, A.; Rahimpour, M. R. A novel configuration for hydrogen production from coupling of methanol and benzene synthesis in a hydrogen-permselective membrane reactor. *Int. J. Hydrogen Energy* **2009**, *34*, 5091–5107.

(5) Khademi, M. H.; Rahimpour, M. R.; Jahanmiri, A. Differential evolution (DE) strategy for optimization of hydrogen production, cyclohexane dehydrogenation and methanol synthesis in a hydrogen-permselective membrane thermally coupled reactor. *Int. J. Hydrogen Energy* **2010**, *35*, 1936–1950.

(6) Setinc, M.; Levec, J. Dynamics of a mixed slurry reactor for the three-phase methanol synthesis. *Chem. Eng. Sci.* **2001**, *56*, 6081–6087.

(7) Rahimpour, M. R.; Elekaei Behjati, H. Dynamic optimization of membrane dual-type methanol reactor in the presence of catalyst deactivation using genetic algorithm. *Fuel Process. Technol.* **2009**, *90*, 279–291.

(8) Rahimpour, M. R.; Elekaei, H. Enhancement of methanol production in a novel fluidized-bed hydrogen-permselective membrane reactor in the presence of catalyst deactivation. *Int. J. Hydrogen Energy* **2009**, *34*, 2208–2223.

(9) Rahimpour, M. R.; Lotfinejad, M. A comparison of auto-thermal and conventional methanol synthesis reactor in the presence of catalyst deactivation. *Chem. Eng. Process* **2008**, *47* (12), 2121–2130.

(10) Rahimpour, M. R.; Parvasi, P.; Setoodeh, P. Dynamic optimization of a novel radial-flow, spherical-bed methanol synthesis reactor in the presence of catalyst deactivation using differential evolution (DE) algorithm. *Int. J. Hydrogen Energy* **2009**, *34*, 6221–6230.

(11) Graaf, G. H.; Scholtens, H.; Stamhuis, E. J.; Beenackers, A. A. C. M. Intra-particle diffusion limitations in low-pressure methanol synthesis. *Chem. Eng. Sci.* **1990**, *45*, 773–783.

(12) Graaf, G. H.; Sijtsema, P. J. J. M.; Stamhuis, E. J.; Joosten, G. E. H. Chemical equilibrium in methanol synthesis. *Chem. Eng. Sci.* **1986**, *41*, 2883–2890.

(13) Jeong, B. H.; Sotowa, K. I.; Kusakabe, K. Catalytic dehydrogenation of cyclohexane in an FAU-type zeolite membrane reactor. *J. Membr. Sci.* **2003**, *224*, 151–158.

(14) Itoh, N. A membrane reactor using palladium. *AIChE J.* **1987**, *33*, 1576–1578.

(15) Moulijn, J. A.; Tarfaoui, A.; Kapteijn, F. General aspects of catalyst testing. *Catal. Today* **1991**, *11*, 1–12.

(16) Iordanidis, A. A. *Mathematical Modeling of Catalytic Fixed Bed Reactors*; Twente University Press: Enschede, The Netherlands, 2002.

(17) Dautzenberg, F. M. *Characterization and Catalyst Development: An Interactive Approach*; Bradley, S. A., Gattuso, M. J., Bertolacini, R. J., Eds.; ACS Symposium Series 411; American Chemical Society: Washington, DC, 1989; Chapter 11, pp 99−119.

(18) Reid, R. C.; Sherwood, T. K.; Prausnitz, J. *The Properties of Gases and Liquids*, 3rd ed.; McGraw−Hill: New York, 1977.

(19) Lindsay, A. L.; Bromley, L. A. Thermal conductivity of gas mixture. *Ind. Eng. Chem.* **1950**, *42*, 1508–1510.

(20) Cussler, E. L. *Diffusion, Mass Transfer in Fluid Systems*; Cambridge University Press: Oxford, U.K., 1984.

(21) Wilke, C. R. Estimation of liquid diffusion coefficients. *Chem. Eng. Progress* **1949**, *45*, 218–224.

(22) Smith, J. M. *Chemical Engineering Kinetics*; McGraw−Hill: New York, 1980.

(23) Shampine, L. F.; Reichelt, M. W. The MATLAB ODE Suite. *SIAM J. Sci. Comput.* **1977**, *18*, 1–12.

(24) Jeong, B. H.; Sotowa, K. I.; Kusakabe, K. Modeling of an FAU-type zeolite membrane reactor for the catalytic dehydrogenation of cyclohexane. *Chem. Eng. J.* **2004**, *103*, 69–75.

(25) Koukou, M. K.; Chaloulon, G.; Papayannakos, N.; Markatos, N. C. Mathematical modeling of the performance of non-isothermal membrane reactors. *Int. J. Heat Mass Transfer* **1997**, *40*, 2407–2417.

(26) Rezaie, N.; Jahanmiri, A.; Moghtaderi, B.; Rahimpour, M. R. A comparison of homogeneous and heterogeneous dynamic models for industrial methanol reactors in the presence of catalyst deactivation. *Chem. Eng. Process* **2005**, *44*, 911–921.

(27) *Operating data sheets of methanol plant*; Shiraz Petrochemical Complex: Shiraz, Iran, 2000−2003.